Xiujun Du[1*]

Automatic Testing Technology of BTB Liquid Crystal Display Advanced Fault Detection in Smart Meter for Smart Machine

Journal of Electrical Systems

Abstract: - In smart meter technology, the reliability of Backplane to Bezel (BTB) Liquid Crystal Displays (LCDs) is crucial for efficient functioning within intelligent grid systems. Defects in these LCD screens can significantly impact overall smart meter performance, necessitating effective detection methods for proper management and utilization. Current detection approaches, which combine manual and automatic methods based on machine vision, have shown unsatisfactory performance. This research addresses this challenge by proposing a novel method for advanced fault detection in BTB LCDs of smart meters, Automatic Testing Technology of BTB Liquid Crystal Display Advanced Fault Detection in Smart Meter for smart machine (BTB-LCD-FD-MCDSGAN) is proposed. The study begins by collecting datasets specifically tailored for LCD screen localization and defect detection. To enhance data quality, a Window Adaptive Extended Kalman Filter (WAEKF) is applied during preprocessing for noise removal. Feature extraction follows, utilizing Parameterized Multi Synchrosqueezing Transforms (PMST) with a primary focus on Gray Level Co-occurrence Matrix features. These extracted features serve as input for classification by a Multimodal Contrastive Domain Sharing Generative Adversarial Network (MCDSGAN), categorizing defects into five types likes normal display, no display, abnormal display, liquid crystal rupture, and incomplete display. Furthermore, the proposed method optimizes the MCDSGAN weight parameter using the Red Fox Optimization Algorithm (RFOA) to achieve accurate LCD fault defect prediction. The entire approach is implemented in Python, performance metrics likes accuracy, precision, recall, F-score, computational time are thoroughly analyzed. Performance of proposed BTB-LCD-FD-MCDSGAN approach attains 20.89%, 33.67% and 25.98% high accuracy, and 17.98%, 23.78% and 33.45% higher recall compared with existing methods such as automatic detection of display defects for smart meters depend on deep learning (AD-AM-DL), deep learning-enabled image content-adaptive field sequential color LCDs by mini-LED backlight (DL-AFSC-LCD) and new multi category defect detection method depend on convolutional neural network technique for TFT-LCD panels (MDF-CNN-LCD), methods respectively.

Keywords: Liquid Crystal Displays, Smart Meter, Red Fox Optimization Algorithm, Parameterized Multi Synchrosqueezing Transforms, Multimodal Contrastive Domain Sharing Generative Adversarial Network.

I. INTRODUCTION

The identification of defects in LCD screens is a crucial aspect of the quality certification process for smart meters throughout their life cycle [1]. Currently, manual methods are predominantly employed for detecting defects in LCD screens of smart meters. However, this approach becomes impractical due to the extensive use of smart meters in power grids. [2-4] have introduced the utilization of template matching methods for defect detection LCD screens of smart meters [5]. While this method demonstrates satisfactory results by detecting defects in input images comprising only LCD screen area, it exhibits poor robustness and becomes ineffective when the size of the LCD screen in smart meters deviates from that of the template. Additionally, accurately identifying and positioning the LCD screen within natural scenes poses a significant challenge [6].

Presently, research focused on localizing LCD screens in smart meters primarily relies on methods such as LSD (Line Segment Detector) [7], [8] or Hough Transform [9]. While these approaches demonstrate satisfactory accuracy in localizing LCD screens with a complete appearance, challenges arise when the target screen exhibits cracks. In such cases, the identification accuracy of the model may be compromised. Additionally, difficulties arise when the input image contains numerous linear edge features, making challenging to automatically filter LCD screen's edge using LSD or Hough Transform methods. Currently, DL methods demonstrated remarkable success in realm of feature extraction, target finding, target recognition research [10]. Here, suggests employing DL method forlocalization of LCD screens, the detection of defects in smart meters. Through extraction of features from input images of smart meters, the deep learning model is capable of pinpointing and identifying defects LCD screens of smart meters with varying sizes. Itimproves method's robustness, diminishes impact of external environmental factors on its performance.

[1] Electronic Information & Artificial Intelligence College, Yibin Vocational & Technical College, Yibin, Sichuan, 644100, China
[*]Corresponding Author Email: 18283189099@163.com

The main contribution of this paper is,

- By collecting datasets specifically designed for LCD screen localization and defect detection, ensuring that the data is representative of real-world scenarios.
- The Window Adaptive Extended Kalman Filter (WAEKF) is employed during preprocessing to enhance data quality by effectively removing noise from the collected datasets.
- The use of Parameterized Multi Synchrosqueezing Transforms (PMST) for feature extraction, with a primary focus on GLCM features. These features capture important characteristics of the LCD screens, aiding in the identification of defects.
- The proposed method utilizes a Multimodal Contrastive Domain Sharing Generative Adversarial Network (MCDSGAN) for defect classification. This approach allows for effective categorization of defects into five types likes normal display, abnormal display, no display, liquid crystal rupture, incomplete display.
- It compares performance of proposed technique by existing approaches, demonstrating significant improvements. Specifically, the proposed approach achieves higher accuracy and recall compared to methods such as AD-AM-DL, DL-AFSC-LCD, and MDF-CNN-LCD.

Remaining part of this paper is arranged below: section 2 defines related work, section 3 designates proposed methodology, section 4 proves outcome with discussion, section 5 designates conclusion.

II. RELATED WORK

Here we review the recent papers of Backplane to Bezel Liquid Crystal Display using deep learning as shown as below;

Chen et al. [11] have introduced two-stage deep learning system that integrates YOLOv5 and ResNet34. YOLOv5 was employed for the localization of smart meter LCDs, while ResNet34 is utilized for classifying LCD faults. To facilitate model training and evaluation, two datasets were created: one for LCD screen localization and another for defect detection. The model demonstrates an impressive defect detection accuracy of 98.9% on dataset specifically designed, showcasing its ability to accurately identify common defects in LCD screens. It has high accuracy but has less precision.

Zou et al. [12] have introduced deep learning for image classification enables precise identification of the optimal Field Sequential Color (FSC) algorithm, characterized by the lowest Color Break-Up (CBU). Furthermore, the algorithm exhibits heterogeneity, as it independently conducts image classification in each segment, ensuring the minimization of CBU across all segments. The validation process encompasses both objective and subjective assessments for comprehensive evaluation. It has low computational time but it has low accuracy.

Ho et al. [13] have introduced a system for detecting the depth of rib marks on TFT-LCDs, comprising three key components likes hardware, system control, software. In hardware section, utilized line scan camera paired by telecentric coaxial lens for imaging. To enhance characteristic information, employed internal coaxial white light source in conjunction by white line light source. The system control aspect involved the use of Nvidia Xavier AGX. It has high precision and also has low accuracy.

Chang et al. [14] have introduced multicategory classification method employing CNN for automating optical inspection (AOI) in the identification of defective pixels on TFT-LCD panels. In presence of a significant class imbalance, with non-defective pixels outnumbering defective ones, posed a substantial challenge. The study showcases efficacy, effectiveness of method using real panel images supplied with mobile manufacturer in Taiwan. It has high sensitivity and also has low f-score.

Zhu et al. [15] have introduced a framework dedicated to robustly addressing module-level defects detection under complex scenarios. The presented framework was built upon the YOLOV3 detection unit and comprises key components such as preprocessing module, defects definition module, detection module, interferences elimination module. Notably, this work marks the first attempt at designing practical AOI scheme specifically tailored for module-level defects detection. To validate efficacy of suggested technique, extensive experimentations were conducted on manufacturing lines. Assessment of AOI system's detection presentation, when compared to a manual scheme, demonstrates the practicality of the system for accurately detecting module-level defects. It attains high f1-score and low precision.

Torres et al. [16] have introduced collaborative project involving UFAM/CETELI, Envision, ICTS, present automated system for detecting mura defects on LCD displays. The system relies on histogram comparisons and

employs ML process known as RF. To assess effectiveness of technique, compare it with the widely used k-Nearest Neighbors (kNN) method. It has high recall but also has low precision.

III. PROPOSED METHODOLOGY

This study introduces an Automatic Testing Technology for Liquid Crystal Display (LCD) Advanced Fault Detection in Smart Meters for Intelligent Grid Systems. The proposed approach, named BTB-LCD-FD-MCDSGAN, employs an optimized Multimodal Contrastive Domain Sharing Generative Adversarial Network. The process begins with the collection of datasets for LCD screen localization and defect detection. Noise removal is performed using a Window Adaptive Extended Kalman Filter (WAEKF) during preprocessing to improve data quality. Feature extraction utilizes Parameterized Multi Synchrosqueezing Transforms (PMST) with a focus on GLCM features. These extracted features are employed for classification with Multimodal Contrastive Domain Sharing Generative Adversarial Network (MCDSGAN) to categorize defects into five type's likes normal display, abnormal display, no display, liquid crystal rupture, and incomplete display. The weight parameter of MCDSGAN is further optimized using the Red Fox optimization algorithm (RFOA) to enhance the accuracy of LCD fault defect prediction. The proposed methodology diagram is shown in Figure 1.

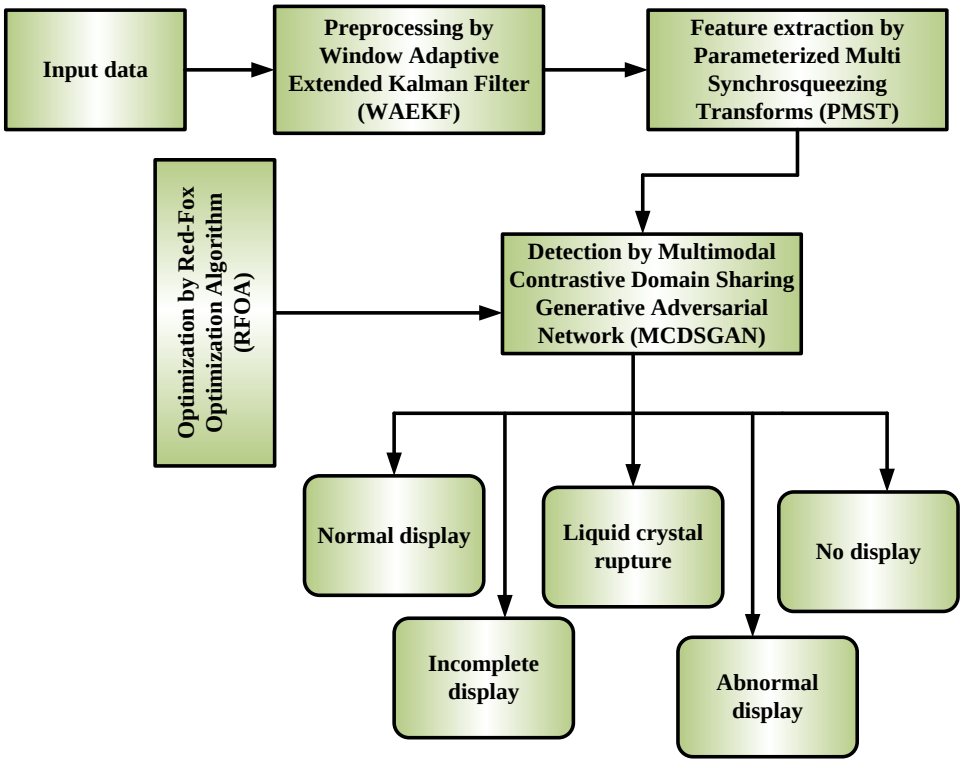

Figure 1: Proposed Methodology Diagram BTB-LCD-FD- MCDSGAN

A. Preprocessing by Window Adaptive Extended Kalman Filter (WAEKF)

The WAEKF [17] is a signal processing technique used for noise removal in preprocessing to improve the quality of data. It is an extension of traditional EKF that adapts to changing conditions within a specified window of data. The WAEKF is particularly effective when dealing with non-stationary signals or when the underlying dynamics of the system may vary over time. The mathematical representation of the WAEKF involves equations for prediction and update steps, similar to the EKF.

Let's denote the state vector as x_k at time k, the measurement vector as z_k, and the process and measurement models as $f(.)$ and $h(.)$ respectively.

The prediction step is given by in equation (1) and (2),

$$\hat{x}_{k|k-1} = f(\hat{x}_{k-1|k-1}) \tag{1}$$

$$P_{k|k-1} = F_k P_{k-1|k-1} F_k^T + Q_k \tag{2}$$

where, $\hat{x}_{k|k-1}$ is the predicted state, $P_{k|k-1}$ is the predicted covariance matrix, F_k is the jacobian matrix of the process model, and Q_k is the process noise covariance matrix.

The update step involves using equation (3) (4) and (5),

$$K_k = P_{k|k-1} H_k^T (H_k P_{k|k-1} H_k^T + R_k)^{-1} \tag{3}$$

$$\hat{x}_{k|k} = \hat{x}_{k|k-1} + K_k (z_k - h(\hat{x}_{k|k-1})) \tag{4}$$

$$P_{k|k} = (I - K_k H_k) P_{k|k-1} \tag{5}$$

Where, K_k denotes kalman gain, H_k signifies jacobian matrix of measurement model, R_k denotes measurement noise covariance matrix. Then preprocess data fed in to Parameterized Multi Synchrosqueezing Transforms for feature extraction.

B. Feature extraction by parameterized local maximum synchrosqueezing transforms (PLMST)

In this section, the parameterized local maximum synchrosqueezing transform (PLMST) [18] for extracting GLCM textual features such as contrast, energy, entropy, homogeneity, and inverse different moments. The mathematical representation of PLMST for feature extraction is given below;

The Parameterized local maximum synchrosqueezing transform (PLMST) has obtained a new TFA method with parameterizing STFT, local maximizing TF reassignment is given in the equation (6),

$$PLMSST(g,\omega',\alpha) = \int_{-\infty}^{+\infty} T(g,\omega,\alpha)\delta(\omega'-\omega_m(g,\omega))q\omega \tag{6}$$

Where, (T) denotes the time (g) is a frequency and (ω) is the block. For multi-component modes, all mono-component mode is decomposed, and TF coefficients in IF trajectories of PLMSST expression is followed in the equation (7).

$$f_x(g) = \frac{1}{2\pi t(0)} PLMSST(g,\varphi'_x(g),\alpha) \tag{7}$$

GLCM features are discussed below

Entropy is scale of disorder of a system. The value of entropy based on mass of system. Entropy have a positive/negative value. Allowing to second law of thermodynamics, entropy of one system decreases only if entropy of another system increases.

$$S(Y, f) = -\sum_z \sum_{a=u} \left[h(z-u, a-k) \log^2 (h(z-y, a-d)) \right] \tag{8}$$

where, $z-u$ signifies spatial relationship of pixels, $a-d$ signifies intensity values , k denotes coordinates of points. Homogeneity refers to degree of uniformity among sampling units within a population. It is often perceived as indicating that the items in identical traits. It is image's comparison variation of co-occurrence matrix. It is given in equation (9).

$$\mathrm{U} = \sum_{\mathrm{v}=1}^{\mathrm{A}} \sum_{\mathrm{x}=1}^{\mathrm{A}} \frac{\mathrm{GLCM}(\mathrm{v},\mathrm{x})}{1+|\mathrm{v}-\mathrm{x}|} \tag{9}$$

here, $v-x$ signifies element of co-occurrence matrix. Energy is ability or potential to perform work, exemplified by the capability to move an object through the application of force. It can take on various forms, including electrical, mechanical, chemical, thermal, or nuclear, and has the capacity for transformation from one form to another. Is sum of pixel point in image is given in equation (10)

$$R = \sum_{v=1}^{A} \sum_{x=1}^{A} GLCM(v,x)^2 \tag{10}$$

where, x and v signifies variation in images, A denotes standard deviation of intensity. Contrast typically denotes the noticeable differences among two or more elements, objects, or concepts. The use of contrast is widespread in various contexts, including art, design, literature, and theoretical interest. It is scale of existence of variation in image pixels. It is given in equation (11)

$$\sum_{v=1}^{A} \sum_{x=1}^{A} |v-1|^2 \times GLCM(v,x) \tag{11}$$

where, v and x signifies variation in pixel, A denotes feature value. Then extracted features are then used for classification by MCDSGAN.

C. Classification using Multimodal Contrastive Domain Sharing Generative Adversarial Networks

In this section, the classification using MCDSGAN [19] is discussed. The features extracted using PMST and Gray Level Co-occurrence Matrix (GLCM) serve as input to the MCDSGAN. The generator component of the MCDSGAN may generate synthetic representations of the input features for each defect type. The discriminator component tries to classify between real and generated samples. It is trained to distinguish features associated with different defect types. The contrastive learning aspect helps the model learn to differentiate between features of different defect types. Positive pairs might be features belonging to the same defect type, and negative pairs might be features from different defect types. The entire MCDSGAN is trained in an adversarial manner, with the generator attempting to generate realistic defect features, and the discriminator learning to correctly classify real and generated features. The trained MCDSGAN is then used for classification. Given a set of features, the model predicts the defect type by considering the learned representations. The mathematical representation of MCDSGAN is given below;

During the training process, weights of network are updated depend on combined error by training algorithm (i.e., back-propagation) and it is given in equation (12)

$$ML_{p,q} = -\log \frac{e^{sim(\hat{a}_p, \hat{b}_q)/t}}{e^{sim(\hat{a}_p, \hat{b}_q)/t} + \sum \tilde{a}\beta\tau - e^{sim(\hat{a}_p, \tilde{a}_q)/t}}, \quad \hat{a}_p = y(s(a_p)), \hat{b}_q = y(s(b_q)), \tag{12}$$

where, sim is defined as cosine similarity, $yands$ denotes non-linear boundaries, t signifies temperature parameter. It has been successful in LCD defect classification and image examination challenges. The multimodal contrastive loss is defined as follows equation (13)

$$Lc(R;\rho;t) = \frac{1}{\left|\alpha^{+}\right|} \sum_{\forall (a_p b_p) \in \alpha+} \left[l(a_p, b_p; \rho; t) + l(b_p, a_p; \rho; t) \right] + \frac{1}{\left|\alpha'^{+}\right|} \sum_{\forall (a'_p b'_p) \in \alpha+} \left[l(a'_p, b'_p; \rho; t) + l(b'_p, a'_p; \rho; t) \right] \tag{13}$$

where α^{+} and α'^{+} denotes set of each LCD similar pairs. We form batch by randomly sampling N pairs images $\{a_p, b_q\} N_p = 1$. $\{a_p, b_q\}$ and $\{a'_p, b'_q\}$ are pairs of different edge boundary views of images. While candy edge generator, purposes to make realistic images and adversarial GAN loss LGAN given in equation (14)

$$\begin{aligned} &L_{GAN}(R, Dis_a, Dis_b) = \\ &K_{b \approx jdata(b)} \left[\log DisB(b) \right] + K_{a \approx jdata(a)} \left[\log(1 - DisB(R_y(a)) \right] + \\ &K_{a \approx jdata(a)} \left[\log DisA(a) \right] + K_{b \approx jdata(b)} \left[\log(1 - DisA(R_x(b)) \right] \end{aligned} \tag{14}$$

Additionally, integrating GAN loss with loss is stated to beneficial for reducing blurring, features from paired images, comparable to Pix2Pix, L1-depend translation loss utilized to minimize differences among input, translation LCD images. Form equation (15)

$$L_T(R) = K_{a \approx jdata(a)} \left[\left\| R_x(a) - b \right\| 1 \right] + K_{b \approx jdata(b)} \left[\left\| R_y(b) - a \right\| 1 \right] \tag{15}$$

Finally, reconstructive loss utilized to minimize distance among reconstructed breast image A' (resp., B'), input image A. Three networks had these metrics calculated, one of which was only trained on frontal thermograms formally in equation (16),

$$L_R(R) = K_{a \approx jdata(a)} \left[\left\| R_x(a) - a \right\| 1 \right] + K_{b \approx jdata(b)} \left[\left\| R_y(b) - b \right\| 1 \right] \tag{16}$$

Consequently, the complete loss of DSGANs is given in equation (17)

$$L(R, Dis_a Dis_b) = L_{GAN}(R, Dis_a, Dis_b, A, B) + \xi L_T(R) + \delta L_R(R) + \chi L_C(R, \rho, t) \tag{17}$$

where ξ, δ and χ denotes coefficients of $L_T(R), L_R(R), L_c(R, \rho, t)$ used in classification. Finally, MCDSGAN classifies the defects as normal display, abnormal display, no display, liquid crystal rupture, incomplete display. Red Fox optimization process is used to enhance weight parameters of MCDSGAN for improved prediction accuracy.

1) Optimization using Red Fox optimization algorithm

The weights parameter of MCDSGAN is optimized utilizing RFOA [20]. Here their behaviors were mathematically described as habits, searching food, and hunting, emerging population though escaping from hunters. Importantly territorial habits and then their relation between adult and young among the fox which help those to easily adaptable to various conditions so that they can survive in any changing environment.

Step 1: Initialization.

Initialize the populace of individuals that has a stable count of foxes. Each one is specified in equation (18),

$$\bar{y} = (y_0,\ y_1,\ \ldots\ldots\ y_{n-1}) \tag{18}$$

To distinguish every fox in iteration, introduce $\left(\bar{y}_b^a\right)^T$.

Where, a = total fox, b = coordinate as per the dimensions of solution space. $\bar{y}^a$ = represents the iteration in T .

Step 2: Fitness Function

The new positions are generated by better individuals who stay on newly positions, else they return to prior location (which moves move toward the best location) in equation (19),

$$\left(\bar{y}^a\right)^T = \left(\bar{y}^a\right)^T + \left(\left(\bar{y}^{Best}\right)^T - \left(\left(\bar{y}^a\right)^T\right)\right) \tag{19}$$

where, $\beta \in \left(0, D\left(\left(\bar{y}^a\right)^T, \left(\bar{y}^{Best}\right)^T\right)\right)$ = represents the randomly chosen scaling hyper-parameter set once on iteration for each individuals. Then the fitness function is calculated by equation (20)

$$fitnessfum\ ction = optimizati\ on(\chi\ and\ \gamma) \tag{20}$$

Step3: Randomness Generation:

The movement red fox is observed via radius, which is indicated through 2 parameters: $\alpha \in \langle 0,\ 0.2\rangle$ = is scaling parameter set once on iteration for every individuals to method stochastically varying distance from prey $0 \in \langle 0,\ 2\pi\rangle$ = is chosen to every individuals in equation (21),

$$R = \begin{cases} C\dfrac{\sin(\phi_0)}{\phi_0} & if\ \phi_0 \neq 0 \\ \theta & if\ \phi_0 = 0 \end{cases} \tag{21}$$

where, θ=is taken as a random value amid 0 and 1. And it predetermined one algorithm at the start that interpreted as an impact of unfavorable weather stages like fog, rain.

Step 4: Exploration Phase.

Here, the model is being used during the exploration phase to take everyone's fitness into account. In the suggested approach, say that the ideal candidate has visited the fascinating locations in equation (22),

$$D\left(\left(\bar{y}^a\right)^T, \left(\bar{y}^{Best}\right)^T\right) = \sqrt{\left\|\left(\bar{y}^a\right)^T - \left(\bar{y}^{Best}\right)^T\right\|} \tag{22}$$

where, $\left(\bar{y}^{Best}\right)^T$ = estimate the square of Euclidean distance.

***Step 5*:** Termination

The weight parameter value from MCDSGAN optimized by support of RFOA Algorithm, iteratively repeat the step 3 until halting conditions. Then MCDSGAN classifies defective type into normal display, abnormal display, no display, liquid crystal rupture, incomplete display with higher accuracy.

IV. RESULT WITH DISCUSSION

Experimental outcomes of presented method are discussed. The BTB-LCD-FD- MCDSGAN approach is implemented in python using LCD defect detection dataset. The obtained outcome of the proposed BTB-LCD-FD- MCDSGAN approach is analyzed with existing systems like AD-AM-DL, DL-AFSC-LCD and MDF-CNN-LCD, methods respectively.

A. Performance Measures

To measure performance metrics likes True Negative, True Positive, False Negative, False Positive values are needed. To measure performance metric, True Negative, True Positive, False Negative, False Positive samples are needed.

- True Positives (tp): Instances correctly classified as a specific defect type.
- False Positives (fp): Instances incorrectly classified as a specific defect type.
- False Negatives (fn): Instances of a specific defect type incorrectly classified another class.
- True Negatives (tn): Instances correctly classified not belonging to a specific defect type.

1) Accuracy

Accuracy measures overall correctness of method in predicting defect types, providing a general assessment of classification performance. It is given in equation (23),

$$\frac{tp+tn}{tp+tn+fp+fn} \tag{23}$$

2) Precision

Precision indicates the accuracy of method specifically in identifying particular defect type, minimizing false positives. It is calculated by equation (24),

$$\frac{tp}{tp+fp} \tag{24}$$

3) Recall

Recall measures the model's ability to capture all instances of a specific defect type, minimizing false negatives. It is calculated by equation (25),

$$\frac{tp}{tp+fn} \tag{25}$$

4) F-score

It combines precision, recall, offering single metric balances trade-off among false positives and negatives. It is calculated by equation (26),

$$2\times\frac{\mathrm{Pr}ecision\times\mathrm{Re}call}{\mathrm{Pr}ecision+\mathrm{Re}call} \tag{26}$$

5) Computational Time

It defines time taken by method to execute defect classification on given dataset.

B. Performance analysis

Figure 2 to 6 portrays simulation outcomes of BTB-LCD-FD-MCDSGAN method. Then, the proposed BTB-LCD-FD-MCDSGAN method is compared with existing AD-AM-DL, DL-AFSC-LCD and MDF-CNN-LCD methods respectively.

The comparison of accuracy between proposed, existing methods is presented in Figure 2. The performance of BTB-LCD-FD- MCDSGAN technique results in accuracy that are 20.76%, 35.97%, and 20.67% higher for the classification of normal display, 35.58%, 23.54% 48.83% higher for the classification of no display, 30.76%, 18.43% and 20.89% higher for the classification of abnormal display, 20.76%, 35.97%, and 20.67% higher for classification of liquid crystal rapture and 20.76%, 35.97%, and 20.67% higher for the classification of incomplete display when evaluated to the existing AD-AM-DL, DL-AFSC-LCD and MDF-CNN-LCD methods respectively.

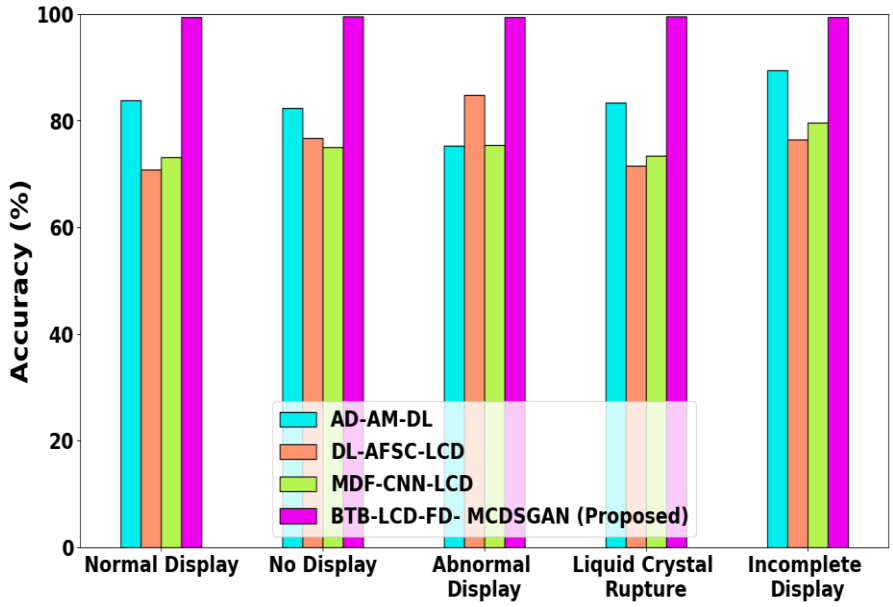

Figure 2: Accuracy analysis

The comparison of precision between proposed, existing methods is presented in Figure 3. The performance of BTB-LCD-FD- MCDSGAN technique results in precision that are 40.76%, 45.97%, and 20.64% higher for the classification of normal display, 25.58%, 23.54% 48.83% higher for the classification of abnormal display, 30.76%, 18.43% and 20.89% higher for the classification of liquid crystal rapture and 20.76%, 35.97%, and 20.67% higher for the classification of incomplete display when evaluated to the existing AD-AM-DL, DL-AFSC-LCD and MDF-CNN-LCD methods respectively.

The comparison of recall between proposed, existing methods is presented in Figure 4. The performance of BTB-LCD-FD- MCDSGAN technique results in recall that are 40.76%, and 40.64% higher for the classification of normal display, 35.58%, 33.54% 48.83% higher for the classification of abnormal display, 20.66%, 18.43% and 20.89% higher for the classification of Cloud server compromise attack, 20.76%, 15.97%, and 23.67% higher for the classification of liquid crystal rapture and 25.76%, 35.97%, and 30.67% higher for classification of incomplete display when evaluated to the existing AD-AM-DL, DL-AFSC-LCD and MDF-CNN-LCD methods respectively.

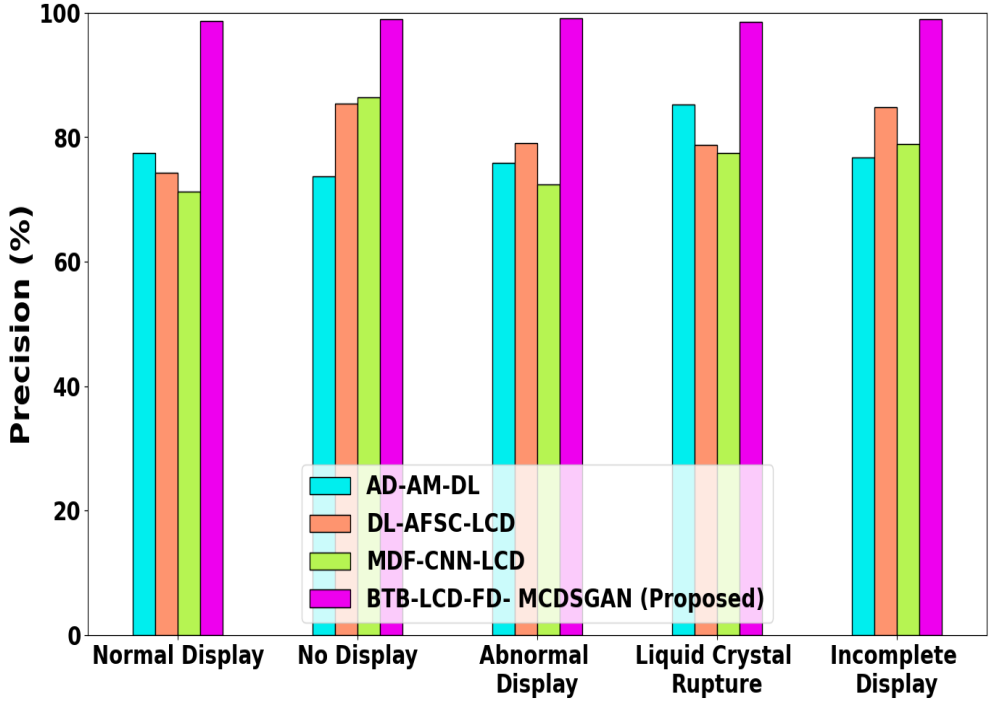

Figure 3: Precision analysis

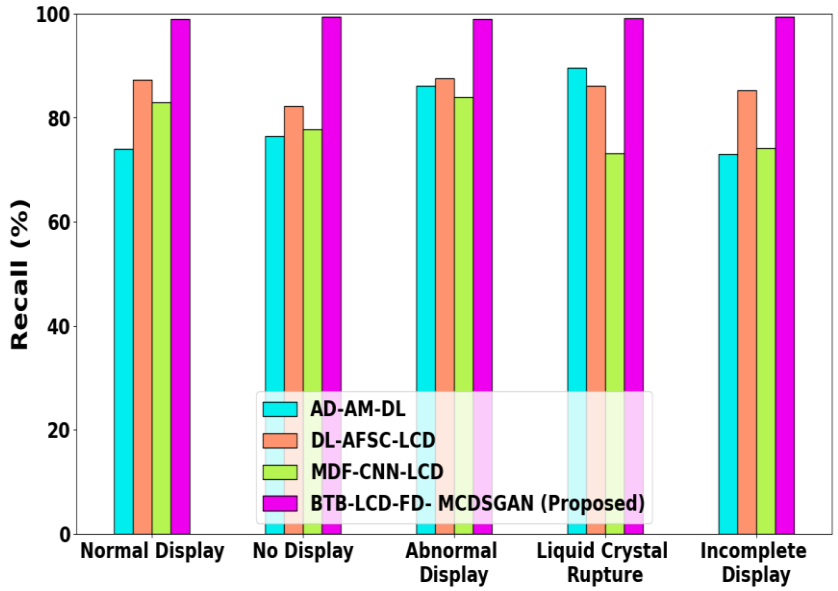

Figure 4: Recall analysis

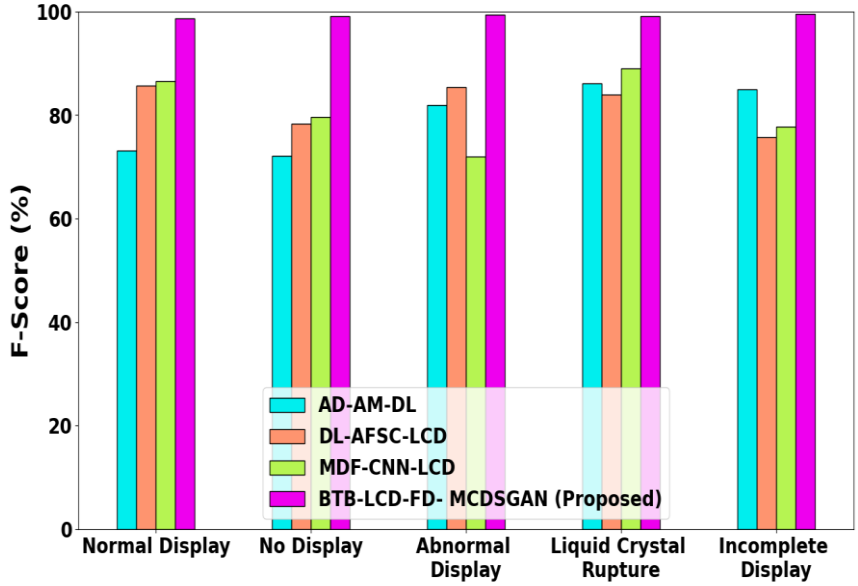

Figure 5: FI-score analysis

The comparison of f-score between proposed, existing methods is displayed in Figure 5. The performance of BTB-LCD-FD-MCDSGAN technique results in f-score that are 40.76%, 30.67% and 40.64% higher for the classification of normal display, 35.58%, 33.54% 48.83% higher for the classification of no display, 20.66%, 18.43% and 20.89% higher for the classification of abnormal display, 20.76%, 15.97%, and 23.67% higher for the classification of liquid crystal rupture and 25.76%, 35.97%, and 30.67% higher for classification of incomplete display when analyzed with existing AD-AM-DL, DL-AFSC-LCD and MDF-CNN-LCD methods respectively.

Figure 6 shows computational time analysis. The BTB-LCD-FD- MCDSGAN is assessed to the AD-AM-DL, DL-AFSC-LCD and MDF-CNN-LCD existing methods. The proposed ATT-LCD-FD-MCDSGAN method provides 5.34%, 10.11%, and 11.20 % lower computational time for classifying the attack detection with existing methods like AD-AM-DL, DL-AFSC-LCD and MDF-CNN-LCD, respectively.

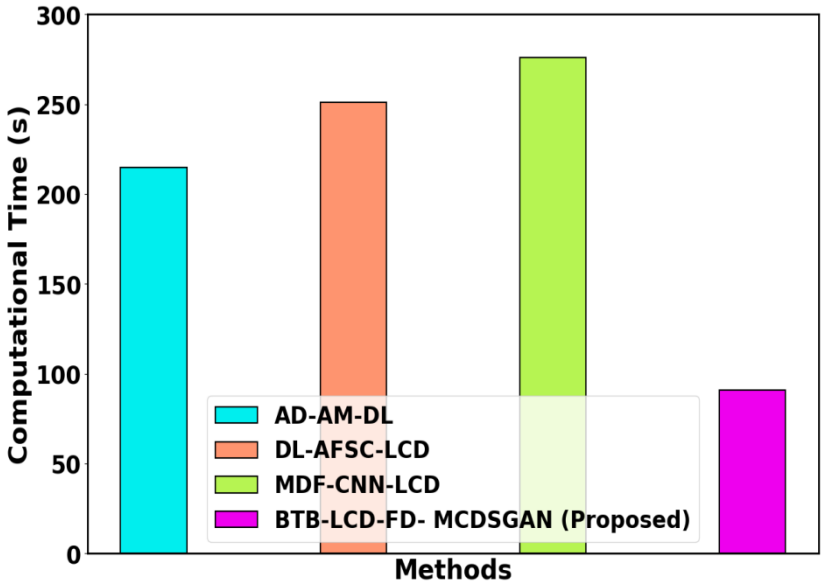

Figure 6: Computational time analysis

Discussion

The proposed research, Automatic Testing Technology of BTB Liquid Crystal Display Advanced Fault Detection in Smart Meter for smart machine (BTB-LCD-FD-MCDSGAN), addresses a critical issue in smart meter technology – the reliable functioning of Backplane to Bezel (BTB) Liquid Crystal Displays (LCDs). The introduction of a novel fault detection method using a combination of advanced technologies demonstrates a significant advancement in improving the accuracy and efficiency of defect detection in smart meters. Let's delve into the key aspects and discuss the implications of this research. The research begins by collecting datasets specifically designed for LCD screen localization and defect detection, indicating a targeted approach for addressing the challenges in smart meter LCDs. The use of the Window Adaptive Extended Kalman Filter (WAEKF) during preprocessing for noise removal indicates a focus on enhancing data quality, which is crucial for accurate defect detection. Utilizing Parameterized Multi Synchrosqueezing Transforms (PMST) with a primary focus on Gray Level Co-occurrence Matrix (GLCM) features showcases a sophisticated feature extraction process for capturing relevant information. The Multimodal Contrastive Domain Sharing Generative Adversarial Network (MCDSGAN) is introduced for defect categorization, distinguishing between five types of defects. This reflects a multi-faceted approach to fault detection. The optimization of the MCDSGAN weight parameter using the Red Fox Optimization Algorithm (RFOA) highlights an effort to fine-tune the proposed method for achieving accurate defect prediction. Investigating the generalizability of the approach to various LCD technologies and smart meter models would contribute to the broader applicability of the proposed method. In summary, the research presents a comprehensive and advanced approach to BTB LCD fault detection in smart meters. The combination of preprocessing techniques, feature extraction methods, and the introduction of MCDSGAN and RFOA for optimization sets the research apart in addressing the challenges associated with LCD defects. Further validation and exploration of scalability and generalizability will be essential for establishing the broader impact of the proposed BTB-LCD-FD-MCDSGAN approach in the field of smart meter technology.

V. CONCLUSION

This study introduces an innovative approach, termed Automatic Testing Technology of BTB Liquid Crystal Display Advanced Fault Detection in Smart Meter for smart machine (BTB-LCD-FD-MCDSGAN). The proposed approach employs a series of advanced techniques, including Window Adaptive Extended Kalman Filter (WAEKF) for noise removal, Parameterized Multi Synchrosqueezing Transforms (PMST) for feature extraction, and Multimodal Contrastive Domain Sharing Generative Adversarial Network (MCDSGAN) for classification into defect types. The MCDSGAN weight parameter optimization is achieved through the Red Fox optimization algorithm (RFOA). Performance evaluation demonstrates the superiority of the proposed ATT-LCD-FD-MCDSGAN approach, achieving significant improvements in accuracy and recall compared to existing methods AD-AM-DL and DL-AFSC-LCD.

Acknowledgement:

2021 Yibin Institute of Vocational Technology School-level Project: "Research on the Application of Board Loading Machine Based on PCB Board Surface Mounting" (ZRKY21YB-25);

2021 Yibin Institute of Vocational Technology Science and Technology Innovation Team Project: "Intelligent Picking Robot Science and Technology Innovation Team" ybzy21cxtd-01

REFERENCE

[1] Inokuchi, T., Okamoto, R., & Arai, N. (2020). Predicting molecular ordering in a binary liquid crystal using machine learning. *Liquid Crystals*, *47*(3), 438-448.

[2] Pessa, A. A., Zola, R. S., Perc, M., & Ribeiro, H. V. (2022). Determining liquid crystal properties with ordinal networks and machine learning. *Chaos, Solitons & Fractals*, *154*, 111607.

[3] Sigaki, H. Y., Lenzi, E. K., Zola, R. S., Perc, M., & Ribeiro, H. V. (2020). Learning physical properties of liquid crystals with deep convolutional neural networks. *Scientific Reports*, *10*(1), 7664.

[4] Xu, Y., Rather, A. M., Song, S., Fang, J. C., Dupont, R. L., Kara, U. I., ... & Wang, X. (2020). Ultrasensitive and selective detection of SARS-CoV-2 using thermotropic liquid crystals and image-based machine learning. *Cell Reports Physical Science*, *1*(12).

[5] Jiang, S., Noh, J., Park, C., Smith, A. D., Abbott, N. L., & Zavala, V. M. (2021). Using machine learning and liquid crystal droplets to identify and quantify endotoxins from different bacterial species. *Analyst*, *146*(4), 1224-1233.

[6] Freitas, R., & Reed, E. J. (2020). Uncovering the effects of interface-induced ordering of liquid on crystal growth using machine learning. *Nature communications*, *11*(1), 3260.

[7] Nayani, K., Yang, Y., Yu, H., Jani, P., Mavrikakis, M., & Abbott, N. (2020). Areas of opportunity related to design of chemical and biological sensors based on liquid crystals. *Liquid Crystals Today*, *29*(2), 24-35.

[8] Lu, H. P., Su, C. T., Yang, S. Y., & Lin, Y. P. (2020). Combination of convolutional and generative adversarial networks for defect image demoiréing of thin-film transistor liquid-crystal display image. *IEEE Transactions on Semiconductor Manufacturing*, *33*(3), 413-423.

[9] Yin, K., Hsiang, E. L., Zou, J., Li, Y., Yang, Z., Yang, Q., ... & Wu, S. T. (2022). Advanced liquid crystal devices for augmented reality and virtual reality displays: principles and applications. *Light: Science & Applications*, *11*(1), 161.

[10] Cui, Y., Wang, S., Wu, H., Xiong, B., & Pan, Y. (2021). Liquid crystal display defects in multiple backgrounds with visual real-time detection. *Journal of the Society for Information Display*, *29*(7), 547-560.

[11] Chen, Y., Hong, Z., Liao, Y., Zhu, M., Han, T., & Shen, Q. (2020). Automatic Detection of Display Defects for Smart Meters based on Deep Learning. *Journal of computing and information technology*, *28*(4), 241-254.

[12] Zou, G., Wang, Z., Liu, Y., Li, J., Liu, X., Liu, J., ... & Qin, Z. (2022). Deep learning-enabled image content-adaptive field sequential color LCDs with mini-LED backlight. *Optics Express*, *30*(12), 21044-21064.

[13] Ho, C. C., Wang, H. P., & Chiao, Y. C. (2021). Deep learning based defect inspetion in TFT-LCD rib depth detection. *Measurement: Sensors*, *18*, 100198.

[14] Chang, Y. C., Chang, K. H., Meng, H. M., & Chiu, H. C. (2022). A novel multicategory defect detection method based on the convolutional neural network method for TFT-LCD panels. *Mathematical Problems in Engineering*, *2022*.

[15] Zhu, H., Huang, J., Liu, H., Zhou, Q., Zhu, J., & Li, B. (2021). Deep-learning-enabled automatic optical inspection for module-level defects in LCD. *IEEE Internet of Things Journal*, *9*(2), 1122-1135.

[16] Torres, G. M., Souza, A. S., Ferreira, D. A., Júnior, L. C., Ouchi, K. Y., Valadão, M. D., ... & Carvalho, C. B. (2021, January). Automated Mura defect detection system on LCD displays using random forest classifier. In *2021 IEEE International Conference on Consumer Electronics (ICCE)* (pp. 1-4). IEEE.

[17] He, Z., Zhang, X., Fu, X., Pan, C., & Jin, Y. (2024). Research on battery state of charge estimation based on variable window adaptive extended Kalman filter. *International Journal of Electrochemical Science*, *19*(1), 100440.

[18] Huang, Z., Wei, D., Huang, Z., Mao, H., Li, X., Huang, R., & Xu, P. (2020). Parameterized local maximum synchrosqueezing transform and its application in engineering vibration signal processing. *Ieee Access*, *9*, 7732-7742.

[19] Zhang, J., Zhang, S., Shen, X., Lukasiewicz, T., & Xu, Z. (2023). Multi-ConDoS: Multimodal contrastive domain sharing generative adversarial networks for self-supervised medical image segmentation. *IEEE Transactions on Medical Imaging*.

[20] Połap, D., & Woźniak, M. (2021). Red fox optimization algorithm. *Expert Systems with Applications*, *166*, 114107.